Pergamon

Int. J. Heat Mass Transfer. Vol. 40, No. 12, pp. 2843–2858, 1997

Printed in Great Britain
0017–9310/97 $17.00 + 0.00

PII: S0017–9310(96)00341–9

High temperature convective drying of wood chips with air and superheated steam

ANDERS JOHANSSON, CHRISTIAN FYHR and ANDERS RASMUSON†

Department of Chemical Engineering Design, Chalmers University of Technology, S-412 96 Gothenburg, Sweden

(*Received* 10 *November* 1995 *and in final form* 16 *September* 1996)

Abstract—High temperature convective drying of single wood chips with air and superheated steam respectively is studied theoretically. The two-dimensional model presented describes the coupled transport of water, vapour, air and heat. Transport mechanisms included are the convection of gas and liquid, intergas as well as bound water diffusion. In the initial part of the drying process, moisture is transported to the surface mainly due to capillary forces in the transversal direction where evaporation occurs. As the surface becomes dry, the drying front moves towards the centre of the particle and an overpressure is simultaneously built up which affects the drying process. The differences between drying in air and superheated steam, respectively, can be assigned to the physical properties of the drying medium. The period of constant drying rate which is comparatively short in air drying becomes more significant with increasing humidity of the drying medium and is clearly visible in pure superheated steam drying. The maximal drying rate is higher in air drying, and shorter drying times are obtained since the heat flux to the wood chip particle increases with increasing amounts of air in the drying medium. The period of falling drying rate can be divided into two parts: in the first, the drying rate is dependent upon the humidity of the drying medium whereas in the second, there is no such correlation. The influence of intergas diffusion in air drying was found to be of minor importance. © 1997 Elsevier Science Ltd.

INTRODUCTION

Biofuels have gained an increasing interest as a fuel source during the past few decades. One reason for this is the environmental advantage over fossil fuels since there is no net emission of either SO_2 and CO_2. One common form of biofuels used for combustion is wood chips. Fresh wood contains a lot of water however, so drying is necessary in order to achieve efficient combustion.

The definition of drying is the removal of a liquid from a material through thermal treatment. The drying process requires a lot of energy, so it is important that it is performed in an optimal way. The main parameters controlling drying are: the temperature and pressure of the drying medium, the slip velocity and, with air as the drying medium, the humidity. Thus, fundamental knowledge of the drying mechanisms is necessary.

The energy required for the evaporation can be supplied to the material in different ways: through conduction, convection, radiation and microwaves. This work focuses on heat transfer to the material via convection and radiation. Convective drying can be carried out at high temperatures, and such high temperature convective drying is an attractive procedure since it has a reduction of the total drying time as its main aim. The drying medium, which traditionally has been hot air, can also be superheated steam at these temperature levels.

The advantages and disadvantages of using superheated steam over hot air as a drying medium in general are discussed by Beeby and Potter [1]. Some of the advantages of using superheated steam mentioned are: the total energy efficiency is increased due to the possibility of reuse of the latent heat of evaporation, the absence of oxygen eliminates the risks of explosions and hazards, and steam drying is simpler to control than air drying. Disadvantages include: problems with temperature-sensitive materials because of the necessity of high temperature levels, difficulties in achieving low moisture contents, and initial condensation which may increase the total drying time of superheated steam drying.

The drying process is usually divided into two different drying regimes: the period of "constant drying rate", where the process is determined by external conditions, and the period of "falling drying rate", where the internal moisture migration limits the drying rate. Drying in the period of constant drying rate with drying media of different humidity (from completely dry air to superheated steam) is thoroughly discussed in the literature [2, 3]. At a certain temperature, referred to as the "inversion temperature", the evaporation rate of water into the drying medium is independent of its humidity. For temperatures above the inversion temperature, the evaporation rate increases with increasing humidity whereas the opposite occurs below this temperature. The inversion

† Author to whom correspondence should be addressed.

NOMENCLATURE

c_p	specific heat capacity [J kg^{-1} K^{-1}]
D	diffusion coefficient [m^2 s^{-1}]
g	acceleration due to gravity [m s^{-2}]
h	external heat transfer coefficient [W m^{-2} K^{-1}] or enthalpy [J kg^{-1}]
H	heat accumulation [J m^{-3}]
j_M	j-factor for mass transfer ($Sc^{2/3}\, k/v_\infty$)
j_H	j-factor for heat transfer ($Pr^{2/3}h/c_p v_\infty \rho$)
k	heat conductivity [W m^{-1} K^{-1}] or external mass transfer coefficient [m s^{-1}]
k_α	relative permeability of phase α [–]
K	absolute permeability [m^2]
L	length [m]
M	mass accumulation [kg m^{-3}]
M_w	molecular weight of water [kg mole^{-1}]
n	mass flux [kg m^{-2} s^{-1}]
Nu_x	Nusselt number (hx/k)
P	pressure [Pa]
P_c	capillary pressure [Pa]
p_v	vapour pressure [Pa]
Pr	Prandtl number ($c_p\mu/k$)
q	heat flux [J m^{-2} s^{-1}]
R	gas constant [J mole^{-1} K^{-1}]
Re_L	Reynold number ($v_\alpha \rho L/\mu$)
Re_x	Reynold number ($v_\alpha \rho x/\mu$)
S	saturation [–]
Sc	Schmidt number ($\mu/\rho D$)
t	time [s]
T	temperature [K]
u	specific internal energy [J kg^{-1}]
v	velocity [m s^{-1}]
x	distance [m]
X	moisture content [kg water/kg dry wood^{-1}]
y	molar fraction [–].

Greek symbols

$\chi_\alpha^{(\kappa)}$	mass fraction of component κ in phase α [–]
ε	emissivity [–] or porosity [–]
μ	dynamic viscosity [kg m^{-1} s^{-1}]
ρ	density [kg m^{-3}]
σ	Boltzmann's constant [W m^{-2} K^{-4}] or surface tension [N m^{-1}].

Subscripts

b	bound or thickness of the wood chip
cr	critical
eff	effective
free	free liquid
FSP	fibre saturation point
g	gas
l	liquid
L	longitudinal
s	surface
sat	saturation
T	transversal
α	phase
0	initial
∞	ambient.

Superscript

a	air
s	surface
w	water
κ	component
∞	ambient.

temperature exists due to combined effects of higher heat transfer coefficients for steam (at the same mass flux) and the depression of the interfacial temperature due to the presence of air in air drying [4]. For evaporation from a horizontal surface into a laminar flow at equal mass flow rates, an inversion temperature of about 250°C is reported [2]. However, the inversion temperature is also dependent on the flow conditions and whether mass or volume flow rates of the drying medium are equalised. At equal volume flow rates the inversion temperature exceeds 400°C [5].

Theoretical and experimental results of the drying of a single spruce chip particle in superheated steam at various conditions are presented by Fyhr and Rasmuson [6]. The aim of this paper is to study the drying when hot air is used as the drying medium and to compare the results with the superheated steam drying. The influence of the humidity at intermediate cases is also studied. To the authors knowledge this has not been done before for the entire drying sequence. The calculations, which include the coupled transport of water, vapour, air and heat, are made with a computer code TOUGH [7] which is modified in order to make simulations of the drying of wood in hot air and superheated steam possible.

TRANSPORT PROCESSES

Wet wood can be considered as a three phase mixture with moisture present in three possible states. The solid cell wall material adsorbs water molecules up to the fibre saturation point (FSP). Above the FSP free liquid partially fills the lumens whereas gas bubbles, consisting of water vapour and air, occupy the remaining lumen space. The moisture content at the fibre saturation point, which indicates the moisture content with no free liquid present, is expressed as [8];

$$X_{FSP} = 0.598 - 0.001T \quad (1)$$

where T is the temperature in Kelvin.

Some assumptions have been made in the calculations. The strong anisotropy of wood makes a two dimensional model necessary. The wood is treated as being homogeneous and no shrinkage of the solid skeleton at low moisture contents is accounted for. Local thermal and phase equilibria exist between the three phases at every point in the particle. The water vapour is saturated above the FSP and the bound water content is a function of temperature only. In the absence of free water, the vapour and the bound water compositions obey the sorption isotherm. A division into external and internal transport is appropriate in the description of heat and mass transport.

External heat transfer

The heat transported from the drying medium to the surface of the wood chip particle is partly by means of convection. For a sharp flat plate, the local convective heat transfer coefficient for a laminar boundary layer is described as [9]:

$$Nu_x = \frac{hx}{k} = 0.332 Re_x^{1/2} Pr^{1/3}. \quad (2)$$

The flow however, is parallel to the large sides of the particle which have a finite thickness, and impinges the end sides. This results in small vortices being formed just behind the edge. Sørensen [10] studied the external mass transfer coefficients experimentally for glass plates with varying thickness covered with naphthalene. The following correlation was adopted from his work:

$$j_M = \frac{k}{v_\infty} Sc^{2/3} = 0.106 Re_L^{-0.25}. \quad (3)$$

By analogy with heat and mass transfer, the external heat transfer coefficient is therefore modelled analogously:

$$j_H = \frac{h}{c_p v_\infty \rho} Pr^{2/3} = j_M \quad (4)$$

and the heat flux to the surface due to convection is:

$$q|_{boundary} = h(T_\infty - T_s). \quad (5)$$

In addition to convection, heat is also transferred to the particle by radiation which is modelled according to the Stefan–Boltzmann law with the emissivity for wood being equal to 0.9. Heat is also transferred due to a simultaneous mass flow across the surface (external mass transport).

Internal heat transfer

Heat transport inside the material occurs via different mechanisms. Transport by conduction is modelled according to Fourier's law (6) with an effective thermal conductivity coefficient accounting for heat conduction in all the three phases. This coefficient, which is determined experimentally, is strongly dependent on the moisture content as well as on the temperature.

$$\mathbf{q} = -k_{eff} \nabla T. \quad (6)$$

Since mass transfer and heat transfer occur simultaneously, heat is also transported by convection. This kind of heat transfer is modelled by weighting the mass fluxes of component κ with the enthalpies as:

$$\mathbf{q} = \sum_{\substack{\alpha = l,g \\ \kappa = a,w}} \mathbf{n}_\alpha^{(\kappa)} h_\alpha^{(\kappa)} \quad (7)$$

where α is the phase.

External mass transfer

In the case of pure superheated steam as the drying medium, there is no convective transport of vapour due to concentration gradients from the surface of the particle to the surroundings since no air is present. When air is present in the drying medium however, this external mass transport must be taken into consideration. The convective mass transfer coefficient necessary for describing this transport is modelled according to equation (3). Consequently, the convective flux of vapour across the boundary is described as:

$$(n_g^{(w)})|_{boundary} = k M_w \frac{P}{RT} (y_g^{(w,s)} - y_g^{(w,\infty)}). \quad (8)$$

In addition to the convective vapour flux mentioned above, another kind of moisture flux is induced in order to equalise the pressure at the surface. This flux is most significant with pure superheated steam as the drying medium.

Internal mass transfer

The transport of fluids through wood can be subdivided into two main categories. Firstly, gas and liquid inside the material is transported by convection through the interconnected voids of the wood structure due to a gradient of the pressure within each phase. For modelling this kind of flow of gas and liquid, respectively, an extended Darcy's law is used:

$$\mathbf{n}_\alpha = -\rho_\alpha K_{sat} \frac{k_\alpha}{\mu_\alpha} (\nabla P_\alpha - \rho_\alpha \mathbf{g}). \quad (9)$$

The relative permeability, k_α, is strongly dependent on the liquid saturation. For moisture contents below the FSP (i.e. no free liquid is present) the relative permeability of the liquid phase is zero and, thus, there is no flux of free liquid. The relative permeability for the gaseous phase is positive for all saturations except for near full saturation where it approaches zero. The pressures of each phase are related to each other via the capillary pressure, P_c, as follows:

$$P_c = P_g - P_l. \quad (10)$$

Consequently, the flux of component κ in phase α due to convection is:

$$\mathbf{n}_\alpha^{(\kappa)} = \chi_\alpha^{(\kappa)} \mathbf{n}_\alpha. \tag{11}$$

Secondly, moisture also migrates via a diffusional mechanism, of which there are two different types. The bound water migration through the cell-wall matrix, which is present for moisture contents below the fibre saturation point, is treated as a diffusion process with the moisture content as the driving force [8]:

$$\mathbf{n}_l^{(w)} = -D_b \nabla X. \tag{12}$$

The unit of the bound water diffusion coefficient is (kg m^{-1} s^{-1}). The other diffusion mechanism is the intergas diffusion of vapour. This transport mechanism is only of interest with air present in the drying medium, and is modelled as:

$$\mathbf{n}_g^{(w)} = -D_{eff} \nabla \rho_g^{(w)} \tag{13}$$

where D_{eff} is the effective diffusion coefficient accounting for the liquid saturation and the tortuosity of the pores.

MATHEMATICAL MODEL

Balance equations

A model using the method of control volumes for simulating the multi-dimensional coupled transport of water, vapour, air and heat in porous and fractured media was developed by Pruess [7] at Lawrence Berkeley Laboratory. The code called TOUGH (transport of unsaturated groundwater and heat) was originally designed for geothermal processes, but the similarities of the governing equations with those present in the drying of wood make the code useful for this application also. The mass balance for each component κ (water and air) is:

$$\frac{\partial M^{(\kappa)}}{\partial t} = \nabla \cdot \left(\sum_{\alpha=l,g} \mathbf{n}_\alpha^{(\kappa)} \right) \tag{14}$$

where the mass accumulation terms are the sums over the gas and liquid phases expressed as:

$$M^{(\kappa)} = \varepsilon \sum_{\alpha=l,g} S_\alpha \rho_\alpha \chi_\alpha^{(\kappa)} \tag{15}$$

and the flux terms are those discussed in equations (9) and (11)–(13).

The saturation of the liquid phase, S_l, is related to the moisture content as:

$$X = \frac{S_l \varepsilon \rho_l}{(1-\varepsilon)\rho_{wood}}. \tag{16}$$

For moisture contents below the FSP, the water is treated as bound water. The energy balance is written as:

$$\frac{\partial H}{\partial t} = \nabla \cdot \Sigma \mathbf{q} \tag{17}$$

where the heat accumulation term H is:

$$H = (1-\varepsilon)\rho_{wood} c_{p,wood} T + \varepsilon \sum_{\alpha=l,g} S_\alpha \rho_\alpha u_\alpha \tag{18}$$

and q is the heat flux calculated from equations (6) and (7).

Initial and boundary conditions

The initial moisture content of the wood chip particle was set to about 1.1 kg/kg (on a dry basis) and the pressure and the temperature were chosen to be 1 bar and 20°C, respectively. The total pressure at the boundaries (using large permeabilities) is equal to the pressure of the drying medium. Across the boundary the fluxes of heat and mass are continuous:

$$\left(\sum_{\alpha=l,g} n_\alpha^{(w)} \right)\Big|_{boundary} = k M_w \frac{P}{RT} (y_g^{(w,s)} - y_g^{(w,\infty)}) \tag{19}$$

$$(\Sigma q)|_{boundary} = h(T_\infty - T_s) + \sigma\varepsilon(T_\infty^4 - T_s^4) + \sum_{\kappa=a,w} n_g^{(\kappa)} h_g^{(\kappa)} \tag{20}$$

and, at a plane of symmetry, the fluxes of mass and heat are zero.

NUMERICAL STUDY

The calculations of high temperature convective drying of spruce chips made are listed in Table 1. The drying medium used in these calculations is either superheated steam ($\chi_g^{(w)} = 1$) or almost dry air ($\chi_g^{(w)} = 0.01$). In order to make an appropriate comparison of the drying process when each of the two drying media is used, the temperature, pressure and flow velocity of the drying medium in each case are equal.

An additional drying parameter must be taken into consideration when drying with air. In a real drying process, the humidity of the drying air changes during the process. Therefore, calculations with various humidity of the drying air are also presented.

The simulated wood chip particle, for which the dimensions are chosen according to Fyhr and Rasmuson [6], is depicted in Fig. 1. The strong anisotropy of wood means that the calculations have to be made for two dimensions, both the longitudinal and the transversal directions. The longitudinal direction must be included in the calculations since its permeability is great compared to those of the other directions. Furthermore, the area available for drying perpendicular to the transversal direction is large when compared to the other surfaces and, thus, this direction must be taken into consideration. The control domain for the calculations covers only one quarter of the total volume of the particle as a result of the symmetry of the wood chip particle.

Table 1. List of calculations

Drying case	Pressure (bar)	Temperature (°C)	Flow velocity (m s^{-1})	Drying medium*
A	1	140	1	air/steam
B	1	160	1	air/steam
C	1	170	1	air
D	1	180	1	air/steam
E	2	170	1	air/steam
F	2	170	2	air
G	3	180	1	air

*air $\rightarrow \chi_g^{(w)} = 0.01$.
steam $\rightarrow \chi_g^{(w)} = 1$.

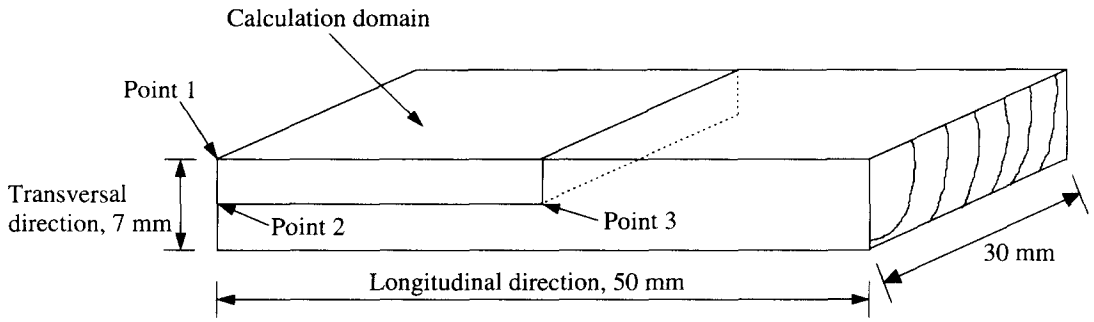

Fig. 1. The wood chip particle used in the simulations.

The equations to be solved are coupled as well as nonlinear and the problem is therefore solved numerically using the method of finite difference. The control domain is discretised into small control volumes (20 in each direction) for which the calculations are made. In Fig. 1 three points of the wood chip particle are specifically marked. These are points for which most of the further discussions are based. The direction of the flow of the drying medium is parallel to the longitudinal direction. The input data including the transport parameters are discussed in the Appendix.

RESULTS AND DISCUSSION

General drying behaviour

Figure 2 shows the typical behaviour of a wood chip particle dried with hot air (Fig. 2(a)) and superheated steam (Fig. 2(b)), respectively (drying case E). The different curves describe the average moisture content, the overpressure in the middle of the particle (point 3) and the temperature at three different points (the three discussed earlier).

In the case of hot air used as the drying medium, it can be clearly seen, that the temperatures of the wood chip tend to approach the wet bulb temperature (61°C) after a very short time. However, the duration at this temperature is very short. This indicates that the surface of the wood chip particle enters the hygroscopic range very quickly, because the internal mass transport is no longer sufficient to keep the surface wet and, thus, the period of constant drying rate almost disappears. The temperatures then increase in a manner reflecting the heat supplied, the moisture movement and the pressure conditions and, when the drying is complete, the temperatures rapidly increase towards the ambient temperature. When the surface enters the hygroscopic range, an overpressure is built up; this overpressure moves simultaneously with the drying front towards the centre of the particle and enhances the transport of moisture in the most permeable direction, which is the longitudinal one. This flux of moisture caused by the overpressure gives rise to a very high moisture content at point 2 which, in turn, keeps the temperature at a low level.

In the case of superheated steam used as the drying medium, on the other hand, there are some important differences to be noted. The temperatures during the period of constant drying rate remain at the boiling point at the operating pressure (about 120°C in this case) compared to the wet bulb temperature in the case of air. In air drying, the local humidity of the gas phase adds an additional degree of freedom giving a more complex temperature behaviour in the intermediate section. The period of constant drying rate proceeds for a considerably longer time when superheated steam is used. This can be explained by two different phenomena. Firstly, during the period of constant drying rate, the moisture transported to the surface is mainly by capillary forces as described by equations (9) and (10). Among the parameters influ-

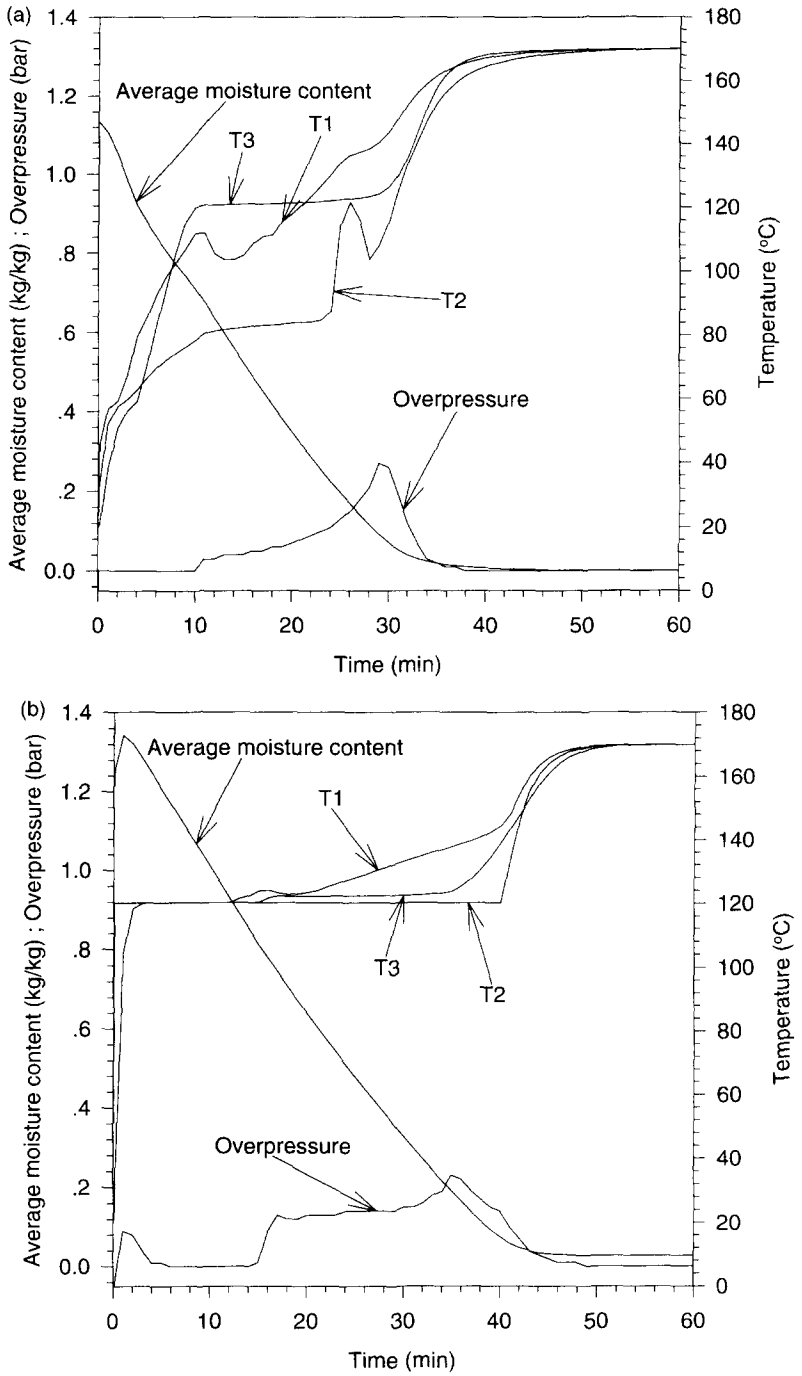

Fig. 2. Drying case E, air (a) and superheated steam (b), respectively.

encing this flux are the density and the viscosity. Together, these parameters are dependent on the temperature in such a way that the mobility of the liquid increases with increasing temperature. Since the boiling point is always higher than the wet bulb temperature, the mobility of moisture is faster in the case with superheated steam than with air and, thus, the surface has a greater tendency to be kept wet. Secondly, for temperatures below the inversion temperature, the convective heat flux with air is higher than with superheated steam due to the greater driving force and, consequently, the surface enters the hygroscopic range faster in the air case.

Another essential discrepancy between the two different drying media is that condensation initially occurs when drying in superheated steam (because of the low initial temperature of the wood chip particle). This condensation leads to an increase of the total drying time which is not negligible and, in order to avoid it, preheating is necessary. It is also notable that

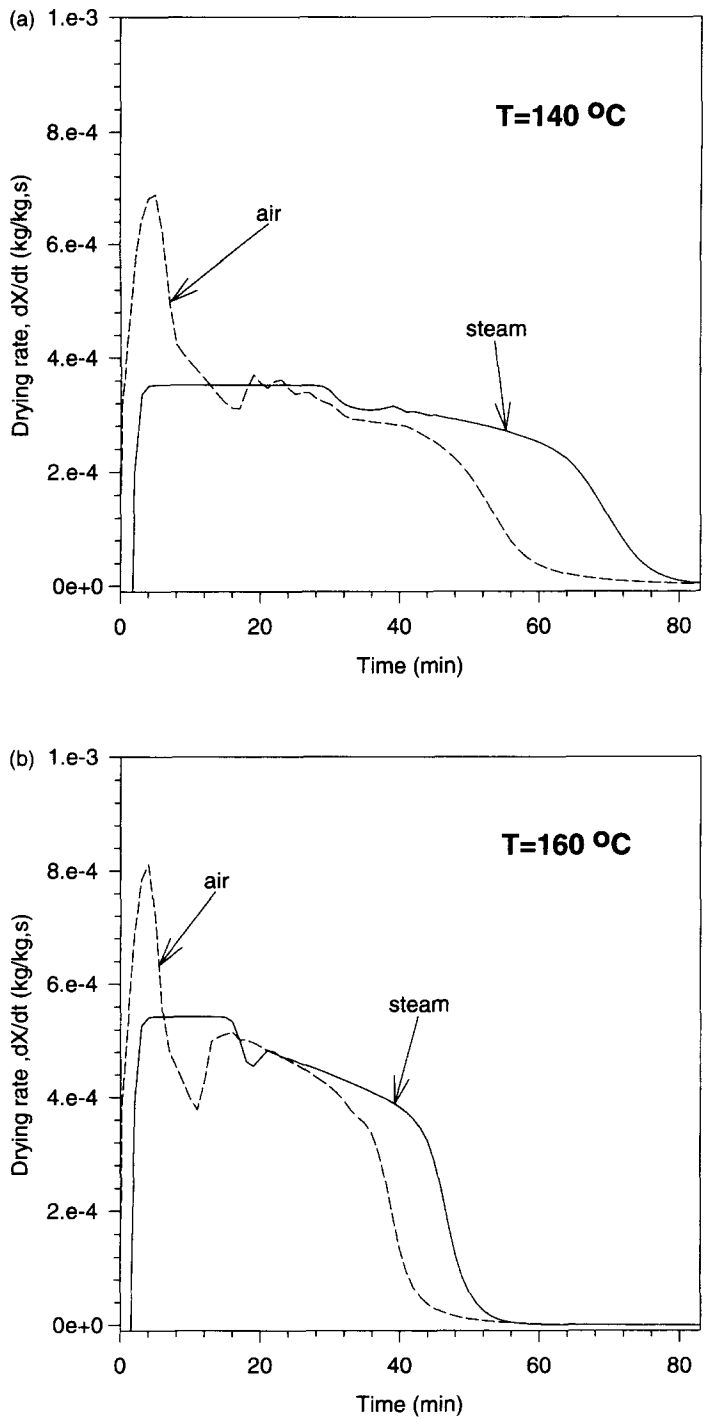

Fig. 3. Drying rates at 140, 160 and 180°C with air and superheated steam, respectively.

the equilibrium moisture content of the wood chip particle is lower in air drying than in steam drying due to the lower relative humidity (or activity) of air as described by the sorption isotherm (see appendix).

Drying rates and drying times

Studies of the drying rate curves at three different temperature levels for the two drying media (Fig. 3) exhibit what has been mentioned earlier. The length of the period of the constant drying rate is considerably longer in the case of superheated steam as the drying medium: with air as drying medium, the existence of this period appears more or less as a "spike". When hot air is used as the drying medium, shorter drying times are obtained and the maximal drying rate (appears in the period of constant drying rate) is greater than with superheated steam as the drying medium. The concept of the inversion temperature

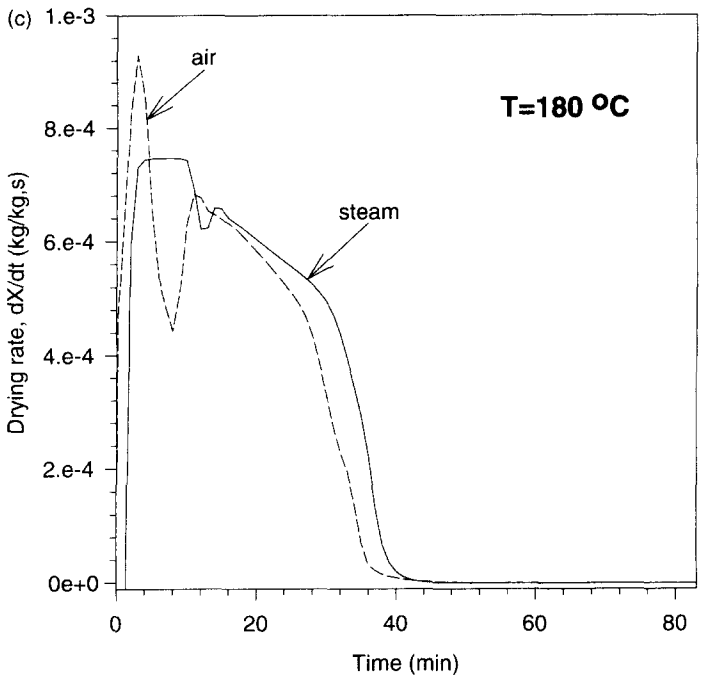

Fig. 3—*continued.*

was discussed in the Introduction of this paper. As already mentioned, the convective heat flux to the wood chip particle from superheated steam and hot air, respectively, during the period of constant drying rate is equal at the inversion temperature. Since the inversion temperature for laminar flow at equal volume flow rates is more than 400°C [5], which more than exceeds the temperature levels used in this study, the convective heat flux when air is used is always higher than that corresponding to superheated steam at these temperatures. However, as depicted in Fig. 3, the differences in the maximal drying rates decrease with increasing temperature of the drying medium, which is an indication of the existence of an inversion temperature. As a consequence of this phenomenon, the differences in the total drying times also diminish.

After the period of constant drying rate, the drying rate rapidly decreases followed by an increase before decreasing further. The increase is a consequence of the internal overpressure which is built up when the surface enters the hygroscopic range. The more severe the drying conditions, the more significant this effect becomes; this also explains the deeper "depression" in the drying rate curve when air is used as the drying medium.

In Figs. 4 and 5 the influence of the temperature, pressure and the flow velocity of the drying air upon the drying rates and drying times are shown. In order to investigate the dependency of the drying temperature the drying rates for drying cases A, B, C and D are plotted vs time in Fig. 4, i.e. all other drying parameters except for the drying temperature are held constant. These results clearly illustrate what should be expected. The total drying time decreases and the maximal drying rate increases with increasing temperature of the drying air. This is consistent with fundamental drying theory since the heat flux from the drying medium to the wood chip particle increases with increasing temperature.

In Fig. 5 the plot of drying cases D and G (Fig. 5(a)) illustrates the dependency of the pressure (1 and 3 bar, respectively) and drying cases E and F (Fig. 5(b)) the dependency of the flow velocity (1 and 2 m s^{-1}, respectively) on the drying time and maximal drying rate. Once again, severe drying conditions, i.e. increased flow velocity and pressure, give rise to shorter drying times and higher maximal drying rates due to increased heat fluxes. When superheated steam is used as the drying medium, increased steam pressure hardly effects the total drying time [6].

Distributions of moisture content and overpressure

Figures 6 and 7 illustrate the distribution of moisture and overpressure throughout the simulated two-dimensional surface at different times for drying case E (with air as the drying medium). The points 1, 2 and 3 which were discussed earlier are also specifically marked out. The visible axes are the exchange surfaces and the concealed ones are the planes of symmetry. The surface perpendicular to the transversal direction starts to dry immediately and, at 4 min, the surface is almost dry. When the surface is completely dry, a drying front moves towards the centre of the particle and, as a consequence of the temperature rise, an overpressure is formed simultaneously (Fig. 7(a)). This overpressure, which moves with the drying front, enhances transport in the most permeable direction, i.e. longitudinal, which explains the enriched amount

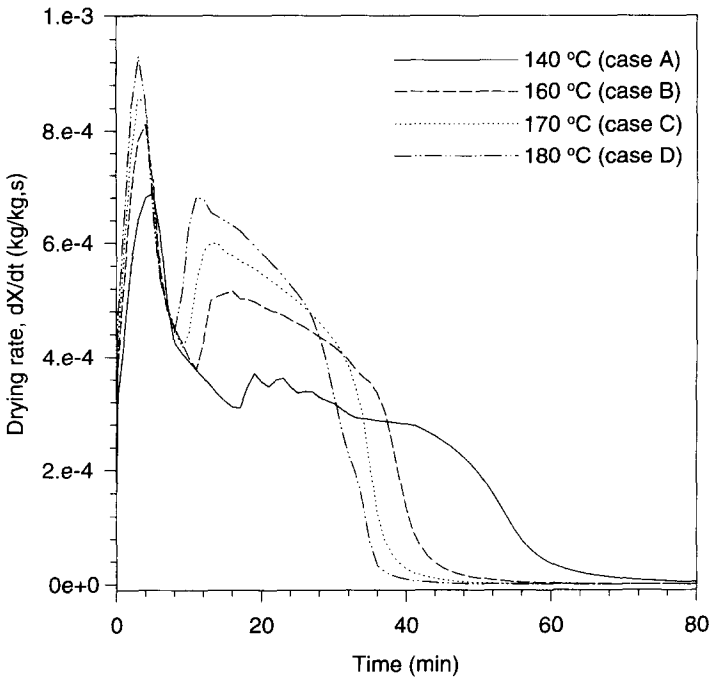

Fig. 4. Temperature dependency of the drying air upon the total drying time and the maximal drying rate.

of moisture at point 2 which can be seen in Fig. 6(b). At 28 min the maximal pressure is close to the centre of the particle and a small remainder of moisture can be seen in the vicinity of point 2 (Fig. 6(c).

Mechanisms of mass transport with time

The importance of different flow mechanisms of moisture during the drying process for drying case E using air is depicted in Figs. 8 and 9. The results are valid for a point in the centre of the calculation domain and the fluxes are regarded as positive towards the surfaces.

In the transversal direction (Fig. 8) the dominating flow mechanism of moisture above the fibre saturation point, which for this domain is reached at about 23 min, is convective flow of liquid. This flow is initially positive due to capillary forces. At 11 min, a strong dip resulting in a convective liquid flux towards the centre occurs which is a result of the overpressure moving with the drying front (see Fig. 7(a)). Simultaneously, the capillary forces become even stronger and, at about 14 min, they are strong enough to compensate for the positive pressure gradient (which pushes the moisture towards the centre) resulting in a positive convective liquid flow. When this point reaches the FSP, the liquid phase becomes discontinuous resulting in zero flux of liquid water. Below the FSP, the diffusion mechanisms dominate, especially the migration of bound water. It is also worth noting the minor importance of the intergas diffusion here.

The fluxes of moisture in the longitudinal direction (Fig. 9) are, in general, larger than the corresponding fluxes in the transversal direction due to the greater permeabilities. This is most significant for the convective gas flow which is negligible in the transversal direction. Just after drying has started, a small maximum of the convective liquid flow can be seen. This is because an initial gradient of the moisture content in the longitudinal direction is formed, causing a capillary flow of liquid towards the surface. However, this gradient quickly diminishes. Then, at about 10 min, the convective flow of liquid rapidly increases as the hump of the overpressure, pushing liquid towards the surface, strongly influences this domain. This increase continues until the relative permeability of the liquid phase in this direction approaches zero as the liquid phase becomes discontinuous (the FSP has, however, not yet been reached since free liquid water still remains in the tapered ends of the tracheids). The diffusion mechanisms in this direction are of minor importance compared to the convective gas flow below the FSP. The negative diffusion flux of bound water is a consequence of the overpressure which pushes the moisture towards the end side, resulting in a negative moisture gradient (see Fig. 6).

Analogous studies for superheated steam drying were made by Fyhr and Rasmuson [6] and the behaviour of the different fluxes are, with some minor differences, similar to those described above for air drying. As mentioned earlier, no intergas diffusion mechanism is present in superheated steam drying but, as discussed above, its influence in air drying is small.

Dependence on the humidity of the drying medium

In air drying, the humidity of the drying air constitutes an additional drying parameter that must be

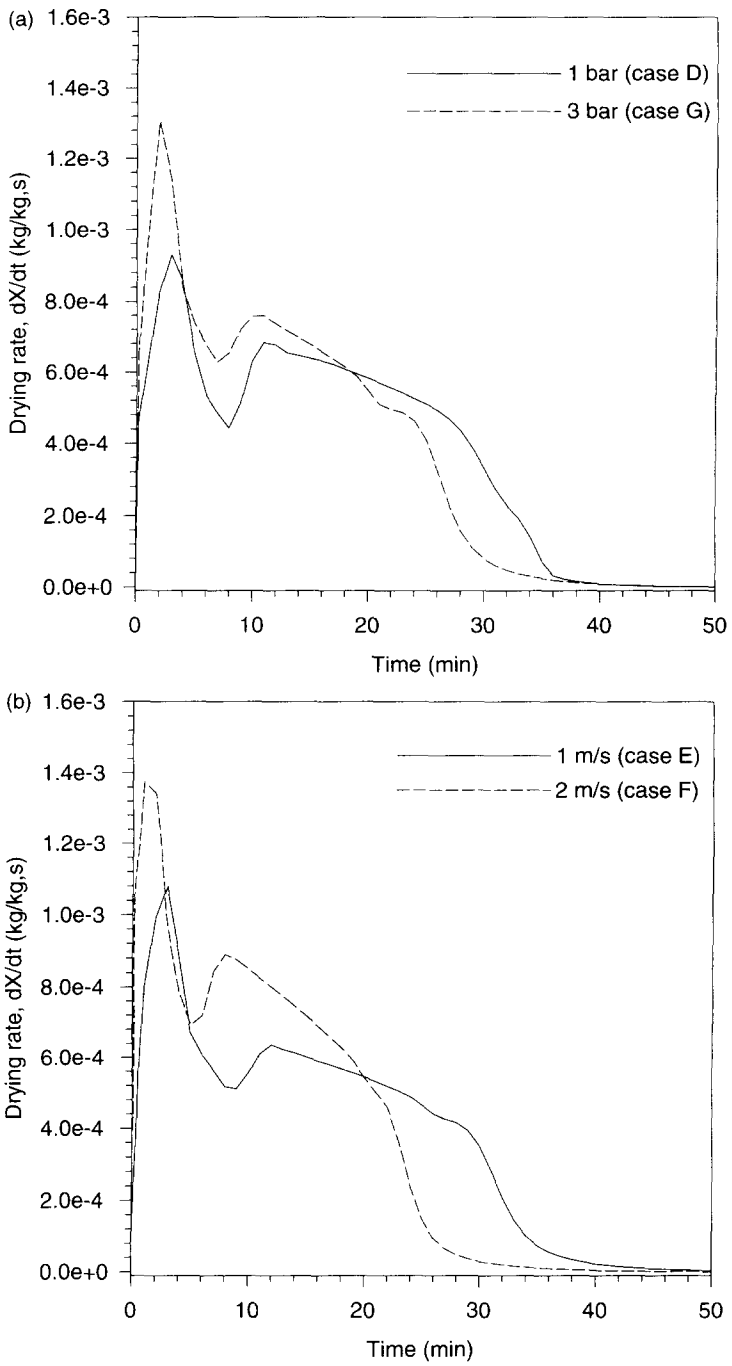

Fig. 5. Dependency on the pressure (a) and the flow velocity (b) of the drying air upon the total drying time and the maximal drying rate.

accounted for. So far, only the extremes have been discussed, i.e. superheated steam ($\chi_g^{(w)} = 1$) and almost dry air ($\chi_g^{(w)} = 0.01$) but, in this section, the humidity of the drying medium is varied between these two values for drying case E in order to investigate its influence.

The drying rates vs time for case E with varying humidity of the drying medium (Fig. 10(a)) show how the period of constant drying rate becomes more significant with increasing humidity of the drying medium: the significance is most obvious in the pure superheated steam case. It is not until the mass fraction of water vapour in the drying medium is increased to about 40% that the drying rate in the first drying period is really constant. The period of falling drying rate starts at the critical moisture content.

When plotting the drying rate vs the average moisture content (Fig. 10(b)) some interesting features are

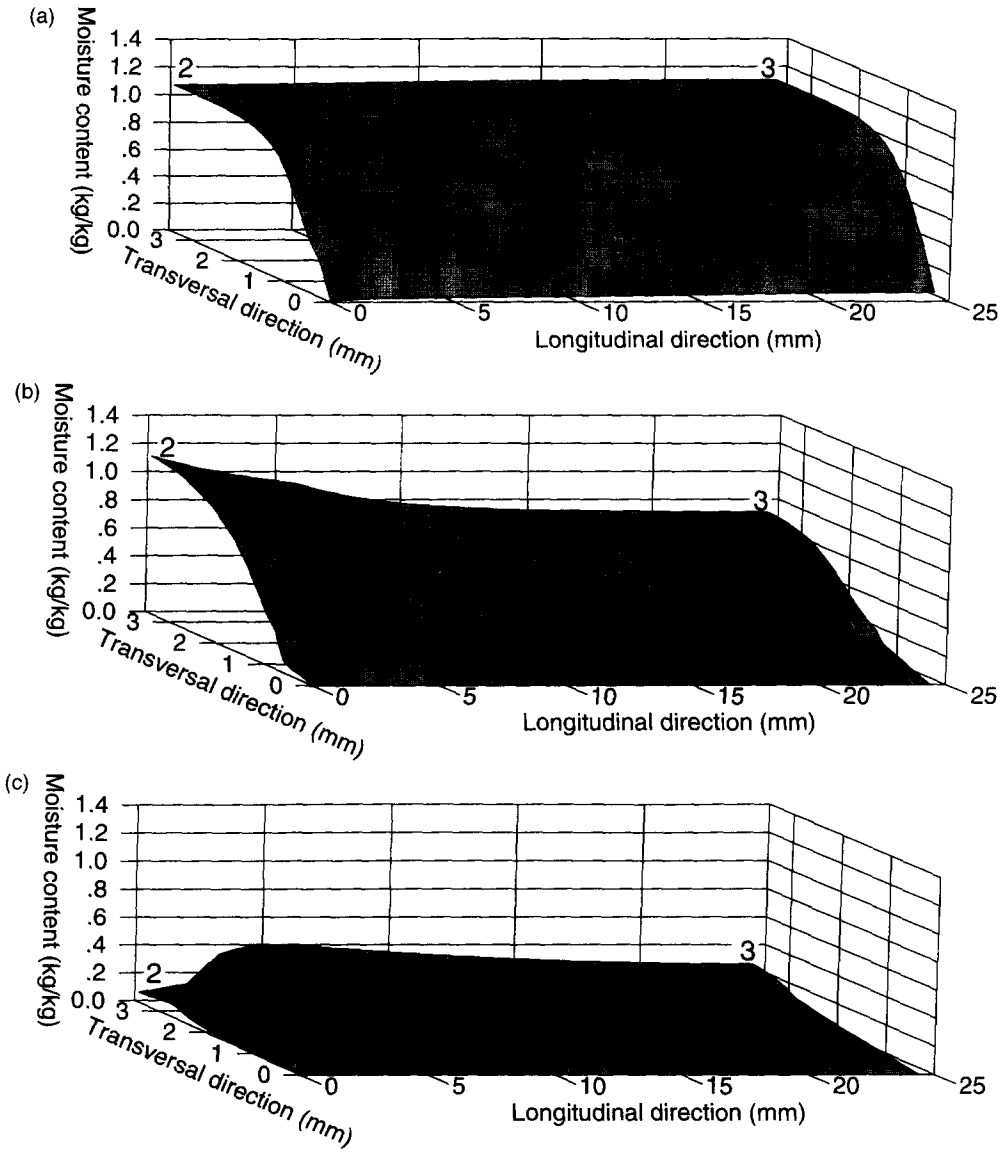

Fig. 6. Distribution of moisture content at 4 min (a), 16 min (b) and 28 min (c).

revealed. As mentioned earlier, the period of constant drying rate is shorter and the maximal drying rate larger with air drying since, in this period, only external drying conditions determine the drying process. In the period of falling drying rate, which can be divided into two parts, the humidity of the drying medium still influences the drying rate in the first part, whereas the drying rate in the second part is independent on the external conditions. The reason for the differences of the drying rates in the first part is explained by the fact that neither external nor internal conditions alone determine the drying rate but rather a combination of both. As a consequence, the dryer the air the faster the drying rate in this part in the period of falling drying rate. This is in contradiction to Faber *et al.*, [5] who expected superheated steam drying to be faster than the air drying in the period of falling drying rate. Once the locally wettest point (point 2) at the surface of the wood chip particle becomes hygroscopic, the drying rate is independent of the external conditions. At this point the second part, where the drying rates are almost equal and independent of the humidity, starts (differences of the drying rate in this part are due to intergas diffusion when air is present). At the end of the drying process, the moisture contents for the different cases differ due to different equilibrium moisture contents resulting from the various humidities of the drying medium.

External mass transfer boundary conditions

As discussed in the literature [11, 12], a difficult task when modelling the external mass transfer is the determination of the external mass transfer coefficient. The problem when drying porous materials, such as

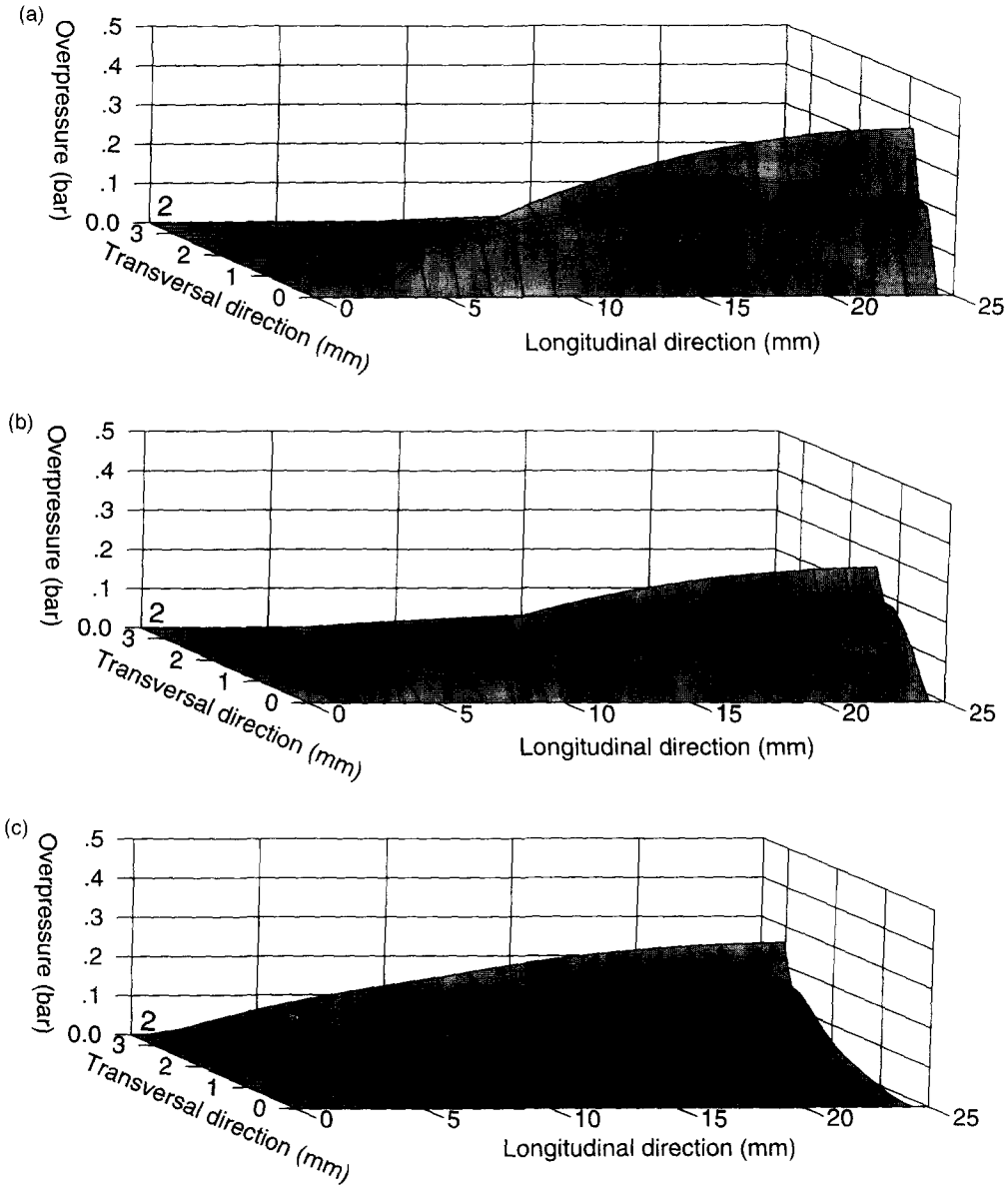

Fig. 7. Distribution of overpressure at 12 min (a), 16 min (b) and 28 min (c).

wood, is that dry patches arise at the surface which, in turn, lead to a decrease in the vapour pressure as discussed by Schlünder [13]. This might affect the external mass transfer coefficient, but its influence is not well understood. Since wood is a hygroscopic material, the decrease in the vapour pressure at the surface for moisture contents below the fibre saturation point is encountered for via the vapour pressure lowering (see appendix). In order to investigate the dependence of the total drying time upon the external mass transfer coefficient, a sensitivity analysis of the external mass transfer coefficient for drying case E with air was performed.

As can be seen from Fig. 11 the total drying time is weakly dependent on variations of the external mass transfer coefficient. A decrease of the coefficient with reference to drying case E by a factor as much as ten only increases the total drying time by 17%, and an increase by a factor of ten only decreases the total drying time by some few percentages.

CONCLUSIONS

A theoretical model describing the drying process of wood chips with hot air and superheated steam respectively is presented. The model is used to investigate the influence of external conditions such as temperature, pressure, flow velocity and humidity on the drying rate, and the moisture content, pressure and temperature within the particle as a function of time.

The differences when drying with air or superheated steam, respectively, can be assigned to the physical

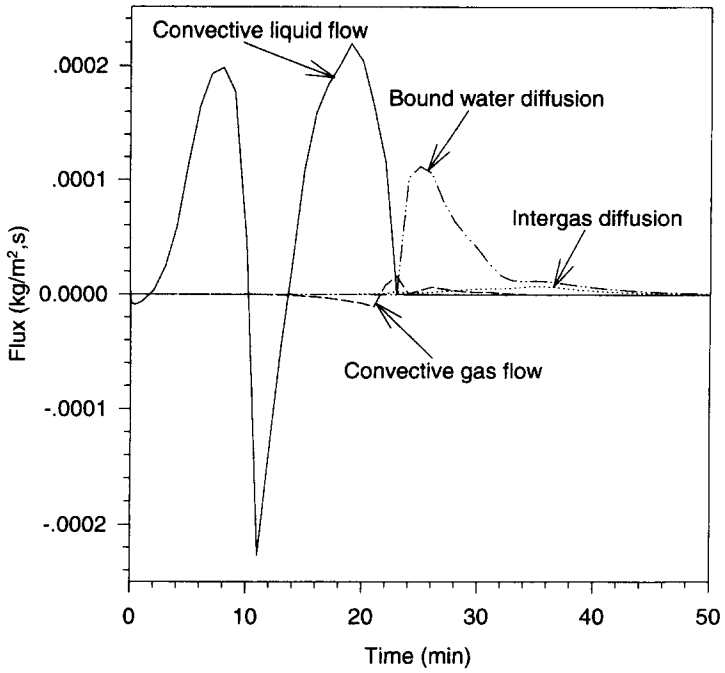

Fig. 8. Different flow mechanisms in the transversal direction

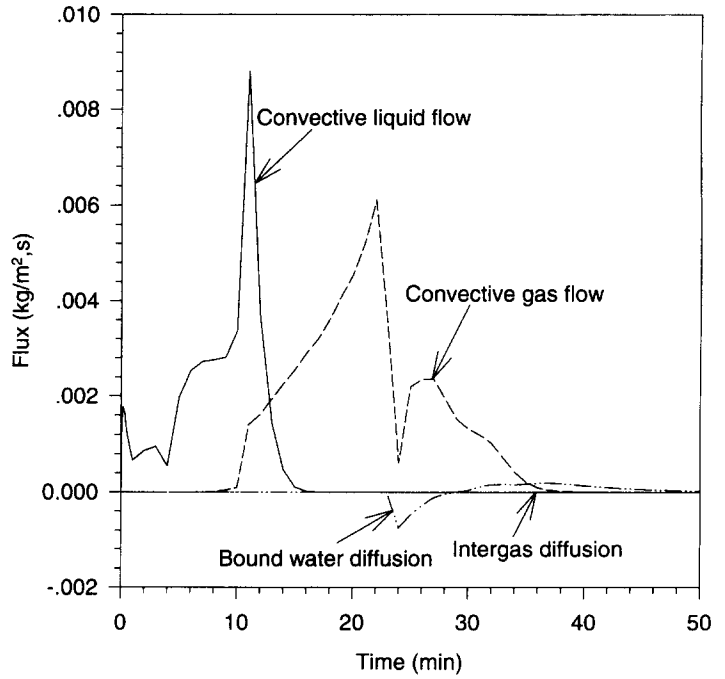

Fig. 9. Different flow mechanisms in the longitudinal direction.

properties of the drying medium. The heat flux from the surroundings to the particle surface is considerably greater when air is the drying medium. This fact, in combination with the lower moisture mobility within the particle (because the wet bulb temperature is lower than the boiling point), results in a much shorter period of constant drying rate since the surface enters the hygroscopic range early in the drying process.

Further on, condensation occurs in superheated steam drying: e.g. for drying case E ($T_\infty = 170°C$, $P_\infty = 2$ bar and $v_\infty = 1$ m s^{-1}) the drying must proceed for about 400 s before the moisture content has

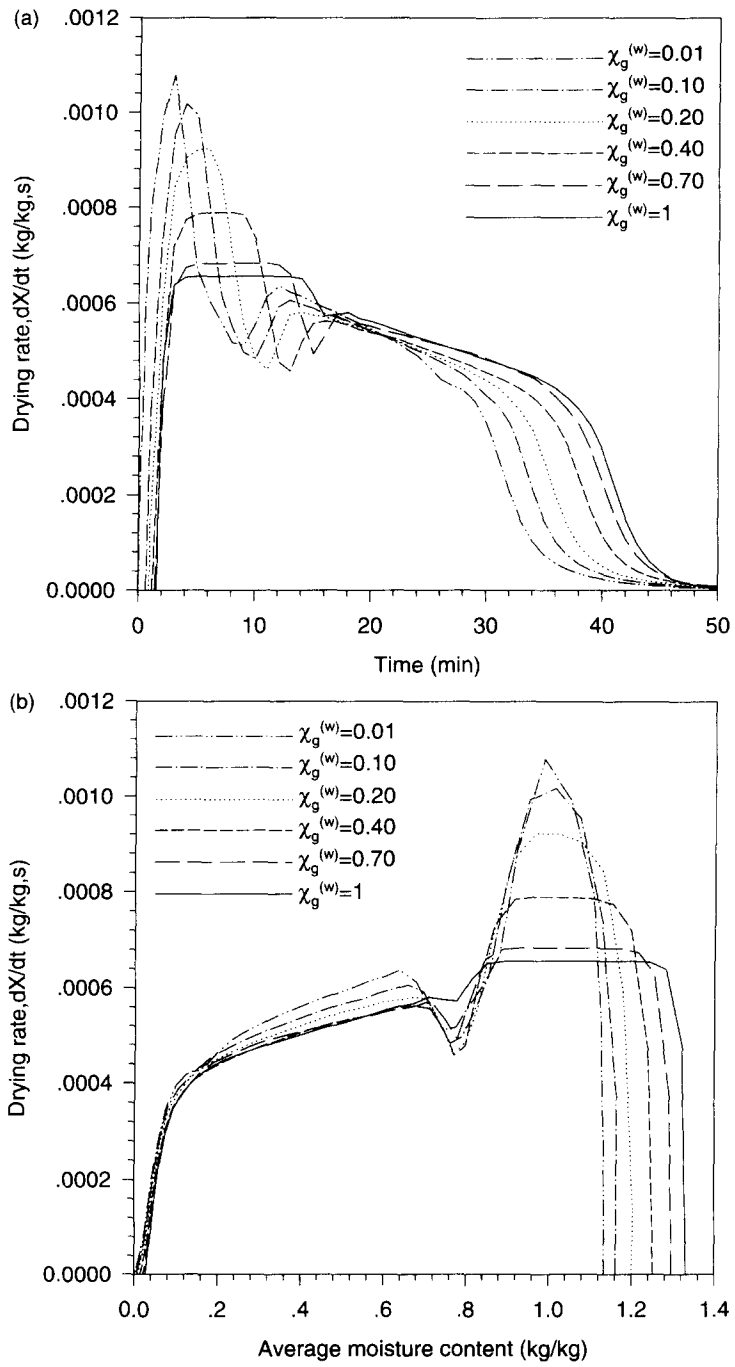

Fig. 10. Drying rates for case E with varying humidity of the drying medium vs time (a) and moisture content (b).

reached the initial moisture content. This, of course increases the total drying time. Preheating is necessary in order to avoid this problem. If very low final moisture contents are required, drying in air is preferred because of the lower relative humidity (activity) compared to superheated steam at the same temperature.

For the temperature levels used in this study (up to 180°C), drying with air gave rise to shorter drying times and higher maximal drying rates than drying with superheated steam. An increase of either the temperature, pressure or flow velocity of the drying air, while keeping the other parameters constant, lead to shorter drying times.

In the initial part of the drying process, the moisture is transported to the surface mainly due to capillary forces in the transversal direction where evaporation

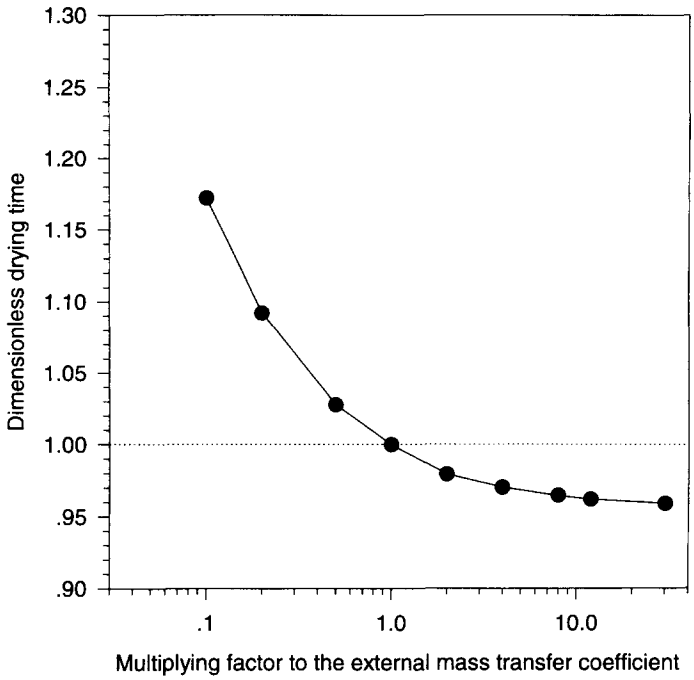

Fig. 11. Dependence of the external mass transfer coefficient on the total drying time.

occurs. When the liquid flow is no longer sufficient to keep the surface wet, the surface becomes hygroscopic and a drying front moves towards the centre of the particle. Simultaneously, an overpressure is built up as the temperature rises. Gas and liquid move in the longitudinal direction as a result of this overpressure. At the end of the drying process, the migration of bound water controls the drying, as the diffusion due to concentration gradients in the gas phase is of minor importance.

A study of the influence of the humidity of the drying medium shows that the period of constant drying rate becomes more significant with increasing humidity of the drying medium. The period of falling drying rate can be divided into two parts: in the first, where an increased humidity of the drying medium leads to lower drying rate, neither external nor internal conditions alone determine the drying rate whereas in the second part, the drying rate is independent on the humidity of the drying medium. A sensitivity analysis showed a weak dependence of the total drying time upon the external mass transfer coefficient.

REFERENCES

1. Beeby, C. and Potter, O. E., Steam drying. In *Drying '85* ed. R. Toei and A. S. Mujumdar. Hemisphere, New York, 1985, pp. 41–58.
2. Chow, L. C. and Chung, J. N., Evaporation of water into a laminar stream of air and superheated steam. *International Journal of Heat and Mass Transfer*, 1983, **26,** 373–380.
3. Sheikholeslami, R. and Watkinson, A. P., Rate of evaporation of water into superheated steam and humidified air. *International Journal of Heat and Mass Transfer*, 1992, **35,** 1743–1751.
4. Mujumdar, A. S., Superheated steam drying: principles, practice and potential for use of electricity. Report no 817 U 671, Canadian Electrical Association, Montreal, Quebec, 1990.
5. Faber, E. F., Heydenrych, M. D., Seppä, R. U. I. and Hicks, R. E., A techno-economic comparison of air and steam drying. In *Drying '86*, ed. A. S. Mujumdar. Hemisphere, New York, 1986, pp. 588–594.
6. Fyhr, C. and Rasmuson, A., Mathematical model of superheated steam drying of wood chips and other hygroscopic porous media. *A.I.Ch.E.Journal*, 1996, **42,** 2491–2502.
7. Pruess, K., TOUGH user's guide, Lawrence Berkeley Laboratory, University of California, Berkeley, CA, 1987.
8. Siau, J. F., *Transport Processes in Wood*, Chap. 6. Springer, Berlin, 1984.
9. Welty, J. R., Wicks, C. E. and Wilson, R. E., Fundamentals of momentum, heat and mass transfer, 3rd edn, Chap. 28. Wiley, New York, 1984.
10. Sørensen, A., Mass transfer coefficients on truncated slabs. *Chemical Engineering Science*, 1969, **24,** 1445–1460.
11. Plumb, O. A., Spolek, G. A. and Olmstead, B. A., Heat and mass transfer in wood during drying. *International Journal of Heat and Mass Transfer*, 1985, **28,** 1669–1678.
12. Salin, J. G., Mass transfer from wooden surfaces and internal moisture non-equilibrium. In *Drying '94*, ed. V. Rudolph, R. B. Keey and A. S. Mujumdar, 1994, pp. 1283–1290.
13. Schlünder, E.-U., On the mechanism of the constant drying rate period. In *Drying '89*, ed. A. S. Mujumdar and M. A. Roques. Hemisphere, New York, 1989, pp. 226–229.
14. Perré, P., Moser, M. and Martin, M., Advances in trans-

port phenomena during convective drying with superheated steam and moist air. *International Journal of Heat and Mass Transfer*, 1993, **36**, 2725–2746.
15. Perré, P. and Degiovanni, A., Simulation par volumes finis des transferts couplés en milieux poreux anisotropes : séchage du bois à basse et à haute température. *International Journal of Heat and Mass Transfer*, 1990, **33**, 2463–2478.
16. Perré, P., Fohr, J. P. and Arnaud, G., A model of drying applied to softwoods : the effect of gaseous pressure below the boiling point. In *Drying '89*, ed. A. S. Mujumdar and M. A. Roques. Hemisphere, New York, 1989, pp. 91–98.
17. Björk, H. and Rasmuson, A., Moisture equilibrium of wood and bark chips in superheated steam. *Fuel*, 1995, **74**, 1887–1890.

APPENDIX

Heat capacity of solid wood	$c_{p,\text{wood}} = 1400\ \text{J kg}^{-1}\ \text{K}^{-1}$
Density of solid wood	$\rho_{\text{wood}} = 1500\ \text{kg m}^{-3}$
Porosity	$\varepsilon = 0.667$
Absolute permeability	
longitudinal	$K_{\text{sat,L}} = 5\times10^{-13}\ \text{m}^2$
transversal	$K_{\text{sat,T}} = 5\times10^{-17}\ \text{m}^2$
Initial moisture content	$X_0 = 1.133$
Humidity of the drying air (when nothing else is mentioned)	$\chi_g^{(w)} = 0.01$.

Heat conductivity [14]

$$X \geqslant 0.4 \quad k_{\text{eff,T}} = \left(\frac{0.65}{100X}+0.0932\right)(1+0.00365\times(T-273.15))(0.986+2.695X)$$

$$X \leqslant 0.4 \quad k_{\text{eff,T}} = (0.129-0.049X)(1+10^{-3}(2.05+4X)\times(T-273.15))(0.986+2.695X)$$

$$k_{\text{eff,L}} = 2k_{\text{eff,T}}$$

Capillary pressure [15]

$$P_c = 1.364\times10^5\sigma(X_{\text{free}}+1.2\times10^{-4})^{-0.63}$$

$$X_{\text{free}} = X - X_{\text{FSP}}.$$

Bound water diffusion coefficient [8]

$$D_{\text{b,T}} = 0.05\frac{D_{\text{BT}}}{(1-\beta)(1-\sqrt{\beta})}$$

$$D_{\text{b,L}} = 5\beta\frac{D_{\text{BL}}}{(1-\beta)(1-\sqrt{\beta})}$$

where

$$D_{\text{BT}} = 0.07\exp\left(\frac{(-9200+7000X)}{R_{\text{gas}}T}\right)$$

$$D_{\text{BL}} = 2.5D_{\text{BT}}$$

$$R_{\text{gas}} = 1.987\ \text{cal mole}^{-1}\ \text{K}^{-1} \text{ and } \beta = 1-0.5(\varepsilon+X).$$

Relative permeabilities
Transversal direction [15]

	k_l	k_g
$X_{\text{free}} = 0$	0	1
$0 < X_{\text{free}} < X_{\text{cr}}$	$0.95\left(\frac{X_{\text{free}}}{X_{\text{cr}}}\right)^2$	$0.95\left(1-\frac{X_{\text{free}}}{X_{\text{cr}}}\right)^2+0.05$
$X_{\text{cr}} < X_{\text{free}} < X_{\text{sat}}$	$0.05\frac{X_{\text{free}}-X_{\text{cr}}}{X_{\text{sat}}-X_{\text{cr}}}+0.95$	$0.05\frac{X_{\text{sat}}-X_{\text{free}}}{X_{\text{sat}}-X_{\text{cr}}}$

$X_{\text{free}} = X - X_{\text{FSP}}$
$X_{\text{free,min}} = 0.$

Longitudinal direction [14]

$$k_l = X^{*8}$$

$$k_g = 1+(4X^*-5)X^{*4}$$

where

$$X^* = \frac{X-X_{\text{FSP}}}{X_{\text{sat}}-X_{\text{FSP}}}.$$

For

$$X^* < 0 \quad k_l = 0 \text{ and } k_g = 1.$$

The permeability of the gas phase in both directions is reduced by a factor of 10 due to pit aspiration.

Effective diffusion coefficient [16]
Transversal direction :

$$D_{\text{eff,T}} = k_g\frac{D_{\text{va}}}{1125}$$

where D_{va} is the diffusion of vapour in air.
Longitudinal direction [14] :

$$D_{\text{eff,L}} = 20D_{\text{eff,T}}.$$

Vapour pressure lowering [17]
For moisture contents below the fibre saturation point, the vapour pressure is lowered as :

$$p_v = \Psi p_{v,\text{sat}}$$

$$C = (1/X_{\text{FSP}}-7.309)/0.1738$$

$$B = -2.575-0.974C$$

$$A = 9.4-0.188B-0.0353C$$

$$\Gamma = \frac{B}{2C}-\frac{1}{2CX}$$

$$\Psi = -\Gamma+\sqrt{\Gamma^2-A/C}.$$